J Oceanogr (2014) 70:521–534
DOI 10.1007/s10872-014-0248-2

ORIGINAL ARTICLE

Synoptic observation of Central Mode Water in its formation region in spring 2003

Eitarou Oka · Kazuyuki Uehara · Toshiya Nakano · Toshio Suga · Daigo Yanagimoto · Shinya Kouketsu · Sachihiko Itoh · Shota Katsura · Lynne D. Talley

Received: 30 January 2014 / Revised: 5 August 2014 / Accepted: 22 September 2014 / Published online: 10 October 2014

Abstract Hydrographic data east of Japan from five research cruises and Argo profiling floats in spring 2003 have been analyzed to examine the relationship of the formation of Central Mode Water (CMW) and Transition Region Mode Water (TRMW) in late winter 2003 to thermohaline fronts and mesoscale eddies. TRMW and the denser variety of CMW (D-CMW) were formed continuously just south of the subarctic frontal zone between 155°E and 165°W with little relation to eddies, suggesting that the absence of the permanent thermocline and halocline in this area is essential for the formation. The lighter variety of CMW (L-CMW) was formed south of the Kuroshio bifurcation front and east of 165°E, partly in an anticyclonic eddy associated with the Kuroshio Extension. Some portion of D-CMW and L-CMW likely had been subducted to the permanent pycnocline by crossing southward the Kuroshio bifurcation front and the Kuroshio Extension front, respectively. In contrast, the formation of these waters in the western regions was inactive and was significantly different from that described previously using multiyear Argo float data. West of 155°E, TRMW and D-CMW were formed only in two anticyclonic eddies that had been detached from the Kuroshio Extension 1–2 years ago. L-CMW was hardly formed west of 165°E, which might be related to the upstream Kuroshio Extension being in its stable state characterized by low regional eddy activity.

Keywords Central Mode Water · Formation · Fronts · Mesoscale eddies · Decadal variability

E. Oka (✉) · D. Yanagimoto · S. Itoh · S. Katsura
Atmosphere and Ocean Research Institute, The University of Tokyo, Kashiwa 277-8564, Japan
e-mail: eoka@aori.u-tokyo.ac.jp

K. Uehara
Department of Marine Science, School of Marine Science and Technology, Tokai University, Shizuoka 424-8610, Japan

T. Nakano
Global Environment and Marine Department, Japan Meteorological Agency, Tokyo 100-8122, Japan

T. Suga
Department of Geophysics, Graduate School of Science, Tohoku University, Aoba-ku, Sendai 980-8578, Japan

T. Suga · S. Kouketsu
Research Institute for Global Change, Japan Agency for Marine-Earth Science and Technology, Yokosuka 237-0061, Japan

L. D. Talley
Scripps Institution of Oceanography, University of California, San Diego, La Jolla, CA 92093-0230, USA

1 Introduction

Central Mode Water (CMW; Nakamura 1996; Suga et al. 1997) is a low-potential vorticity (Q) water formed as the deep winter mixed layer north of the Kuroshio Extension. It is subducted to the permanent pycnocline around the northern edge of the North Pacific subtropical gyre and is then transported anticyclonically in the gyre. Formation, subduction, and circulation of CMW and their temporal variability are important not only physically for the three-dimensional structure of the subtropical gyre (Yasuda and Hanawa 1997), reemergence of winter sea surface temperature anomalies (Hanawa and Sugimoto 2004; Sugimoto and Hanawa 2005), and the maintenance of the Subtropical Countercurrents as well as its impact on the atmospheric circulation (Kobashi and Kubokawa 2012), but also biogeochemically for oceanic uptake of

atmospheric CO_2 and the subsequent CO_2 transportation (Ono et al. 1998; Ishii et al. 2001; Midorikawa et al. 2006), timing and magnitude of spring algal blooms (Shiozaki et al. 2013), and circulation of dissolved organic matter (e.g., Yamashita and Tanoue 2009) and radioisotopes (Aoyama et al. 2008; Rossi et al. 2013).

Investigation of such CMW's roles using observations and/or numerical models requires precise knowledge on the CMW formation and subduction, which has been pursued during the past decade. Oka and Suga (2005) examined the repeat hydrographic section along 165°E to demonstrate that, as suggested by an earlier observation (Mecking and Warner 2001) and an ocean general circulation model (Tsujino and Yasuda 2004), CMW has two varieties: the lighter variety (L-CMW) having $\theta = 11-14°$ C, $S = 34.3-34.6$, and $\sigma_\theta = 25.8-26.2$ kg m^{-3} (θ and σ_θ are potential temperature and density; S is salinity) formed between the Kuroshio Extension front (KEF) and Kuroshio bifurcation front (KBF) and the denser variety (D-CMW) with 8−10° C, 34.0−34.2, and 26.3−26.4 kg m^{-3} formed between the KBF and the subarctic frontal zone (SAFZ). Saito et al. (2007) analyzed a hydrographic survey conducted northeast of Japan in July 2002 to reveal the existence of a colder, fresher low-Q water with 5−7° C, 33.5−33.9, and 26.5−26.6 kg m^{-3} around 43°N, 160°E south of SAFZ, and named it Transition Region Mode Water (TRMW). More recently, Oka et al. (2011a), using Argo profiling float data during 2003−2008, presented that two zonally elongated bands of deep winter mixed layer corresponding to the formation regions of L-CMW and D-CMW/TRMW extend at 33°−39° and 39°−43°N, respectively, from the east coast of Japan to 160°W. The winter mixed layer depth in both bands decreases eastward east of 170°E, implying large-scale eastward CMW subduction by the eastward mean flow between 170°E and 160°W. This agrees with the CMW signature in the subsurface, that is, low-Q distribution on various isopycnals in the subtropical gyre (Oka et al. 2011a).

In spite of such recent progress, the picture of the CMW formation still needs to be updated. The first reason is an unclarified relationship between the CMW formation and thermohaline fronts. While the CMW and TRMW observed in the hydrographic sections were closely associated with the fronts (Oka and Suga 2005; Saito et al. 2007), the overall relationship between the CMW/TRMW formation and the fronts is hard to obtain by statistical analyses of Argo float data (e.g., Oka et al. 2011a). As the most noticeable example, SAFZ is located at relatively low latitudes in the area east of Japan (e.g., Yuan and Talley 1996; Yasuda 2003), thus crossing the western part of the D-CMW/TRMW formation region detected by Argo float observations (fig. 2 of Oka and Qiu 2012). The second reason is the role of mesoscale eddies in the CMW formation. A recent composite analysis of Argo float and altimetric sea surface height anomaly data indicated that thick mode waters are preferentially formed in anticyclonic eddies, particularly in a latitude band between 35° and 40°N corresponding mainly to the L-CMW formation region (Kouketsu et al. 2012). This relationship needs to be further investigated because (1) eddies cannot be distinguished from meanders of fronts in the sea surface height anomaly distributions (Stabeno et al. 2009; Kouketsu et al. 2012), and (2) the eddy field in the CMW formation region exhibits large year-to-year variability, particularly in association with the decadal variability of the Kuroshio Extension (Qiu and Chen 2005, 2011; Qiu et al. 2007). We need to clarify in which particular area the CMW formation occurs (or does not occur) in eddies and how such a formation contributes to the large-scale CMW subduction and its temporal variation.

To examine the relationship of the CMW formation to the fronts and eddies, synoptic observation data with enough zonal/meridional resolution over the CMW formation region are indispensable. Unfortunately, the Argo profiling float data in a particular month alone are insufficient for such purpose, even today when we have more than 3,000 floats in the world oceans with an average float density of 1 per 3° square (Roemmich et al. 2009; Freeland et al. 2010). Alternatively, in this paper, we use shipboard hydrographic data that were intensively collected in the CMW formation region in spring 2003, rather by chance, during five research cruises. The data include those along several meridional sections, which are suitable to reveal the relationship between the CMW formation and the fronts. By analyzing the shipboard hydrographic data supplemented by Argo float data, we examine the relationship of the CMW formation in late winter 2003 to the fronts and mesoscale eddies.

The data are explained in Sect. 2. After determining the location of each front in Sect. 3 and detecting CMW and TRMW in Sect. 4, we described the relationship of these waters to the fronts and eddies in Sect. 5. Discussion is in Sect. 6, and summary is provided in Sect. 7.

2 Data

We used shipboard temperature and salinity data measured by a conductivity-temperature-depth profiler (CTD) and an expendable CTD (XCTD) from five research cruises in spring 2003 (Fig. 1a): the R/V *Kofu-maru* 0304 cruise, the R/V *Seifu-maru* 0304 cruise, and the R/V *Ryofu-maru* 0306 cruise by the Japan Meteorological Agency (2005), the R/V *Hakuho-maru* KH-03-1 cruise by the Ocean Research Institute, The University of Tokyo (Kawabe 2005; Komaki and Kawabe 2009), and the R/V *Shoyo-maru* FY2003 1st

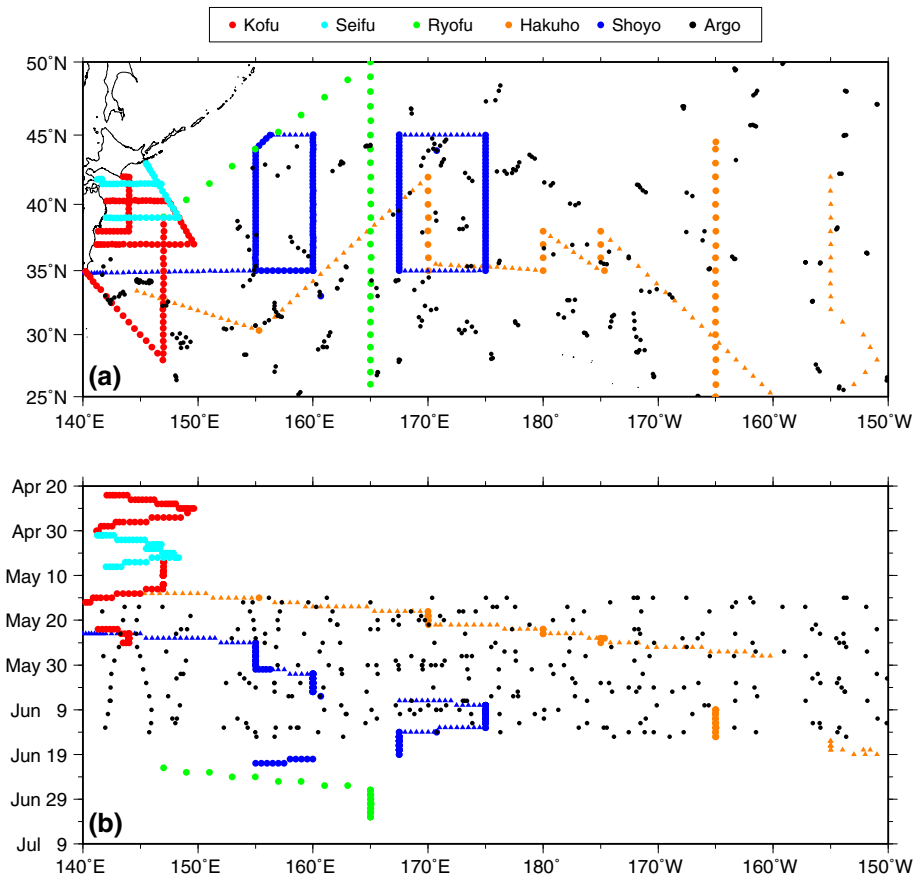

Fig. 1 **a** Distributions of observations conducted by shipboard CTD (*circles*) and XCTD (*triangles*) and Argo floats (*black dots*) in spring 2003. Color of symbols denotes the research cruises. **b** Date of observations shown in (**a**), plotted against longitude

research cruise by the Fisheries Research Agency (Uehara et al. 2004). In the latter two cruises, dissolved oxygen was also measured by the sensor during the CTD casts. The five cruises were conducted between April 22 and July 3, mostly in May and June (Fig. 1b). To supplement the shipboard observations, we added Argo profiling float data in a 1-month period from May 15 through June 15, which were downloaded from the ftp site of the Argo Global Data Assembly Center (ftp://usgodae.org/pub/outgoing/argo, ftp://ftp.ifremer.fr/ifremer/argo) and edited as outlined in Oka et al. (2007). Note that the Argo float density in 2003 was much lower than that in recent years.

We also used delayed-time sea surface height (SSH) and SSH anomaly (SSHA) data merged from TOPEX/Poseidon, Jason, ERS-1/2, and Envisat altimeter observations, produced by Ssalto/Duacs and distributed by AVISO (Ducet et al. 2000). The weekly data, provided on a $0.25° \times 0.25°$ grid, were downloaded from the AVISO web site (http://www.aviso.oceanobs.com).

3 Frontal structure

We first determined the structure of thermohaline fronts in spring 2003. The zonal section at 35°N and meridional sections between 147° and 167.5°E crossed a deep and strong θ and S front near 35°−36°N (Fig. 2). Since this front was associated with the 12° C isotherm at 300 dbar, it was judged to be KEF described in Mizuno and White (1983) and Levine and White (1983). The location of KEF in each section, which was defined as the horizontal θ gradient maximum at 300 dbar, corresponded well to the zonal or meridional SSH gradient maximum (Fig. 3). Accordingly, the KEF distribution on the map was determined so as to correspond to the large horizontal SSH gradient between sections (Fig. 4).

All the meridional sections also exhibited a near-surface density-compensating θ and S front, characterized by the outcrop of 33.2−33.8 isohalines constituting the subarctic permanent halocline (Fig. 2). Based on this structure, the front was judged to be SAFZ studied by Roden (1970, 1972), Zhang and Hanawa (1993), and Yuan and Talley (1996). The location of SAFZ was determined first in each section as the horizontal S maximum at 50 dbar, and then on the map (Fig. 4) using S distribution at that depth (not shown) constructed from our hydrographic observations, in order that the front separates the subtropical water with $S > 33.8$ and the subarctic water with $S < 33.2$.

The meridional sections between 155 and 175°E included another weaker θ and S front between KEF and SAFZ

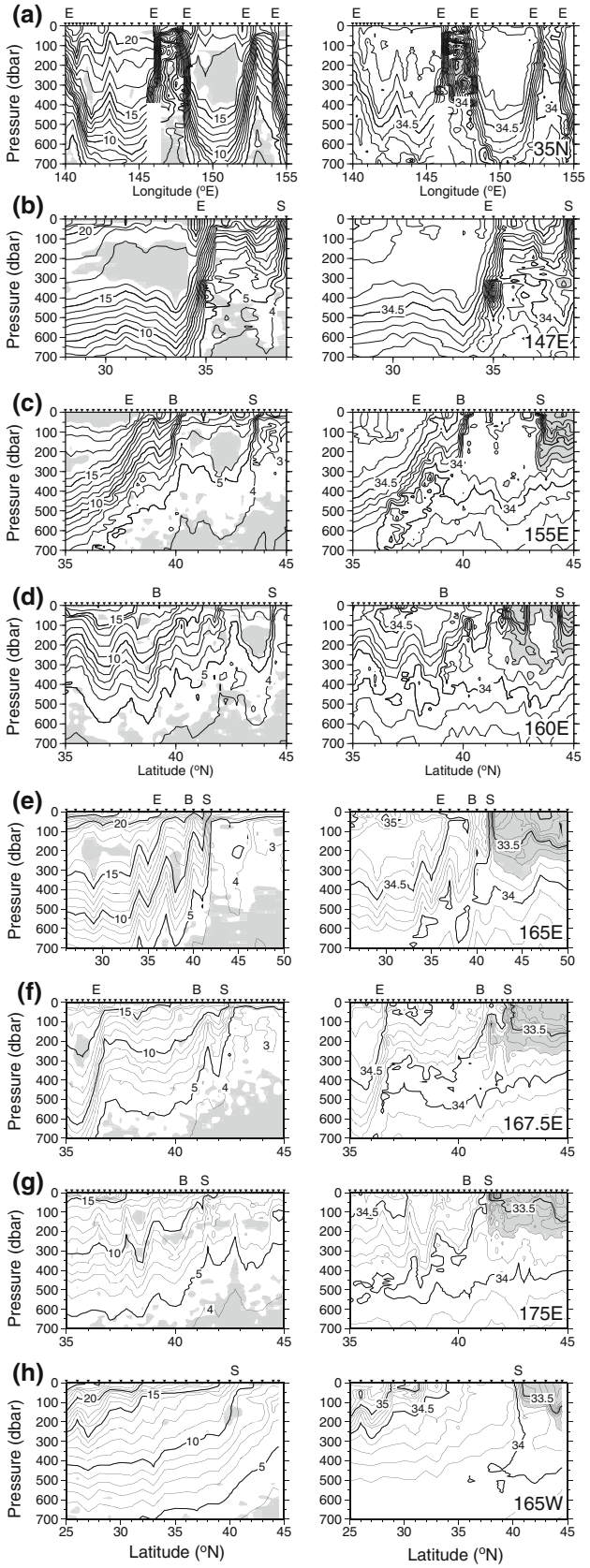

◀**Fig. 2** Distributions of θ (°C; *left*) and S (*right*) in the zonal section at **a** 35°N and the meridional sections at **b** 147°E, **c** 155°E, **d** 160°E, **e** 165°E, **f** 167.5°E, **g** 175°E, and **h** 165°W. *Gray shading* denotes regions of $Q < 1.0 \times 10^{-10}$ m^{-1} s^{-1} (*left*) and $S < 33.8$ (*right*). *Inverted triangles* on the *top of each panel* indicated locations of hydrographic stations. *E*, *B*, and *S* denote the central locations of KEF, KBF, and SAFZ, respectively

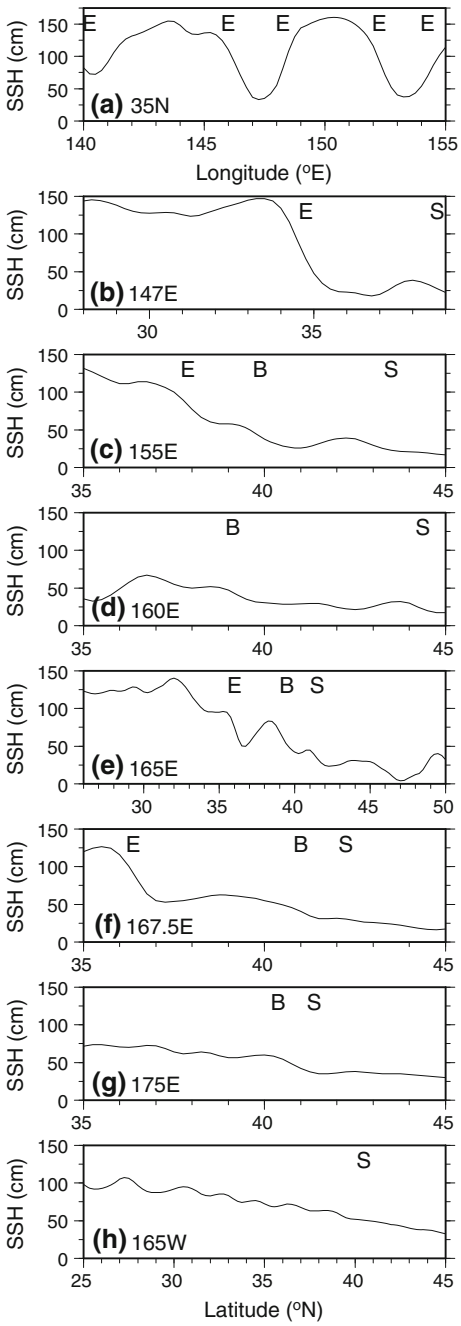

Fig. 3 SSH distributions along the hydrographic sections on the day closest to the hydrographic observations: **a** 35°N on May 21, **b** 147°E on May 7, **c** 155°E on May 28, **d** 160°E on June 4, **e** 165°E on July 2, **f** 167.5°E on June 18, **g** 175°E on June 11, and **h** 165°W on June 11. *E*, *B*, and *S* denote the central locations of KEF, KBF, and SAFZ, respectively

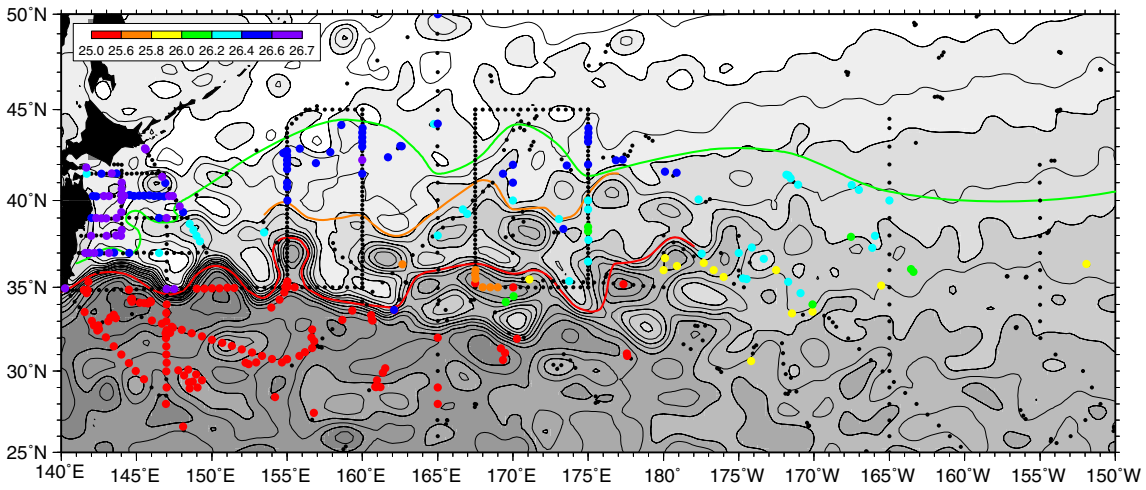

Fig. 4 Distributions of core σ_θ (kg m^{-3}; *color dots*) of pycnostads in spring 2003. The observation points without a pycnostad are indicated by *black dots*. *Red*, *orange*, and *green curves* denote KEF, KBF, and SAFZ, respectively. The *background contours* represent SSH averaged in May–June. The contours are drawn at an interval of 10 cm, with *darker shading* for larger values

(Fig. 2). This front was associated with 6−8° C isotherms at 300 dbar, and was therefore judged to be KBF described in Mizuno and White (1983) and Levine and White (1983). The location of KBF in each section, which was defined as the horizontal θ gradient maximum at 300 dbar, also corresponded to the meridional SSH gradient maximum (Fig. 3). Accordingly, the KBF distribution on the map was determined so as to be aligned with SSH contours (Fig. 4).

In spring 2003, KEF meandered eastward from 140°E, where it left the southern coast of Japan, to a little beyond 180°. The upstream KEF was during its stable period (Qiu and Chen 2005), showing two quasi-stationary meanders with crests at 144° and 150°E, as demonstrated in previous studies (e.g., Kawai 1972; Mizuno and White 1983). In contrast, KEF east of 160°E was surrounded by mesoscale eddies, particularly anticyclonic eddies to its north and cyclonic eddies to its south. This is consistent with Qiu and Chen (2011), who clarified that the downstream KEF fluctuates decadally in the opposite phase with the upstream KEF, being unstable when the upstream KEF is in a stable state.

KBF extended between 155° and 175°E along the northern rim of the anticyclonic eddies. It was supposed to be bifurcated from KEF somewhere between 150° and 155°E. SAFZ left the east coast of Japan at ~36°N and meandered northeastward. It crossed the 160°E section at 44.375°N and extended eastward farther east. In each hydrographic section, it appears as a single, sharp θ/S front (Fig. 2), as previously observed in the western North Pacific (Yuan and Talley 1996).

4 Classification of pycnostads

As the mixed layer in the mode water formation region in the North Pacific becomes deepest in February−April (Oka et al. 2007), we expect that the data analyzed in this study were obtained within 3 months after the mode water formation in late winter 2003 and capture the structure of newly formed mode waters relatively well. To extract such newly formed mode waters from individual CTD/XCTD/Argo profiles, we define a pycnostad in each profile as a layer with $Q < 1.0 \times 10^{-10}$ m^{-1} s^{-1}, a more severe criterion than previous mode water studies (e.g., Oka 2009; Oka et al. 2011a; Saito et al. 2011). Here, Q is defined neglecting relative vorticity (e.g., Talley 1988; Oka et al. 2011b) as

$$Q = gf\frac{\partial\sigma_\theta}{\partial p}, \tag{1}$$

where f is the Coriolis parameter, g the gravity acceleration, and p is pressure. After detecting pycnostads, we exclude ones with thickness <50 dbar, bottom depth <100 dbar, or core $\sigma_\theta > 26.7$ kg m^{-3}. The thickness and bottom depth conditions are imposed to neglect small-scale features and spring mixed layers, respectively. Core properties are defined as properties at the Q minimum, which is considered to be the least modified portion since the pycnostad was formed, thus best preserving the water properties at the time of formation; the core σ_θ condition is imposed because $\sigma_\theta = 26.6$ kg m^{-3} is the densest mixed layer density class in the open North Pacific (e.g., Talley 1993; Oka et al. 2011a).

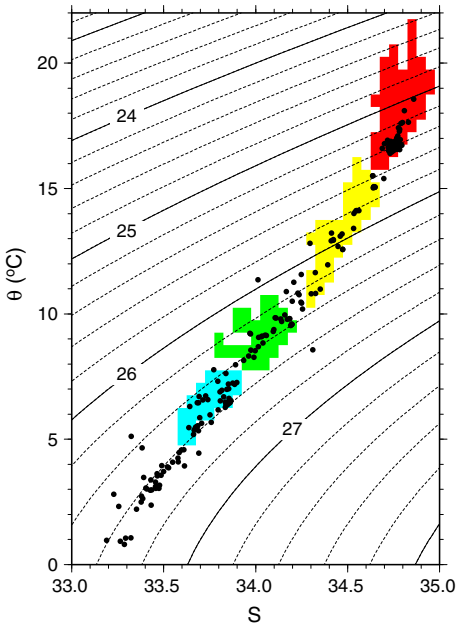

Fig. 5 The θ–S relationship (*dots*) at the core of pycnostads in spring 2003. *Red*, *yellow*, *green*, and *blue shading* indicates properties of STMW, L-CMW, D-CMW, and TRMW, respectively, based on Argo float data in February–April of 2003–2008 (Oka et al. 2011a). *Solid* and *dashed contours* denote σ_θ (kg m^{-3})

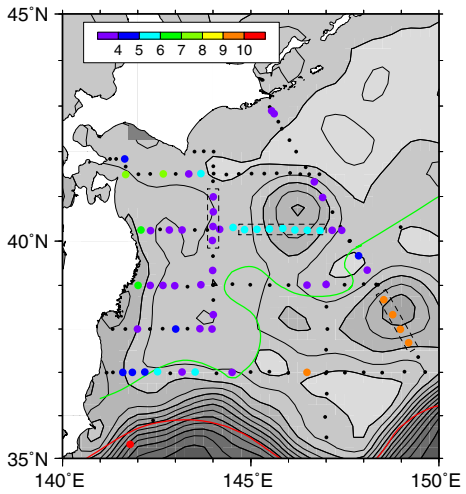

Fig. 6 Distribution of core θ (°C; *color dots*) of pycnostads, constructed mostly from the *Kofu-maru* and *Seifu-maru* cruises in April 22–May 25, 2003. The observation points without a pycnostad are indicated by *black dots*. *Red* and *green* curves denote KEF and SAFZ, respectively. The *background contours* represent SSH on May 7. The contours are drawn at an interval of 10 cm, with *darker shading* for larger values. *Dashed lines* indicate CTD stations used for Fig. 7

Our observations in spring 2003 captured pycnostads with a wide range of core properties: $\sigma_\theta = 25.0-26.7$ kg m^{-3}, $\theta = 1-19°$ C, and $S = 33.2-34.9$ (Figs. 4, 5). Relatively warm and light pycnostads south of KEF and west of 170°E with core $\sigma_\theta < 25.6$ kg m^{-3} were the Subtropical Mode Water (STMW; Masuzawa 1969; Fig. 2b), which was formed in late winter 2003 (Oka and Suga 2003). Most of them had nearly zonally uniform core properties of $\sigma_\theta = 25.35-25.45$ kg m^{-3}, $\theta = 16.5-17.0°$ C, and $S = 34.7-34.8$ (fig. 11 of Oka 2009; Fig. 5). Pycnostads at 35°–36°N, 167°–169°E trapped in an anticyclonic recirculation had core σ_θ of 25.68–25.69 kg m^{-3}, core θ of 15.0–15.1° C, and core S of 34.64–34.65, which were located in a gap between the STMW and L-CMW properties on the θ–S diagram.

Our observations also captured pycnostads colder than 5° C, that is, colder than TRMW (Fig. 5). Most of them were located in the area east of Japan, particularly to the northwest of SAFZ (Fig. 6). These pycnostads were the Oyashio Water, whose low-Q characteristics are attained in the Okhotsk Sea (Ohtani 1989; Kono and Kawasaki 1997; Yasuda 1997). In the Oyashio Water pycnostads including those at 37°N, 142.5°E, 37°N, 143.5°E, and 41.5°N, 143.7°E whose core θ is slightly higher than 5° C, θ and S were stratified, as exemplified in Fig. 7a, indicating that the pycnostads were not formed in the local winter mixed layer. On the onshore side of the Oyashio Water, relatively warm pycnostads with θ of 6–8° C existed near the east coast of Japan at 39°–41°N (Fig. 6). These pycnostads having θ and S similar to TRMW were the Tsugaru Warm Water originating from the Japan Sea (Sugiura 1958; Ohtani 1971).

By excluding the above waters (STMW, Oyashio Water, and Tsugaru Warm Water) and pycnostads whose core properties deviate from CMW/TRMW, a synoptic distribution of CMW/TRMW pycnostads in spring 2003 is obtained (Fig. 8a). Compared to the former distribution (Fig. 4), pycnostads have disappeared in the area east of Japan, except for those associated with either of two anticyclonic eddies centered at 40.5°N, 146°E and 38.5°N, 149°E (Fig. 6). In these pycnostads, θ and S were almost vertically uniform (Fig. 7b, c), in contrast with the Oyashio Water (Fig. 7a), indicating that they originated in the mixed layer in late winter 2003.

5 Distribution of CMW and TRMW in relation to fronts and eddies

In spring 2003, CMW/TRMW pycnostads were distributed between 33° and 44°N, from 145°E to 163°W (Fig. 8a), a geographical range similar to that of the formation region of these waters detected using the 2003–2008 late winter Argo float data (Fig. 4 of Oka et al. 2011a). However, the detailed structure of mode waters is quite different between the two datasets, particularly in the western part of the

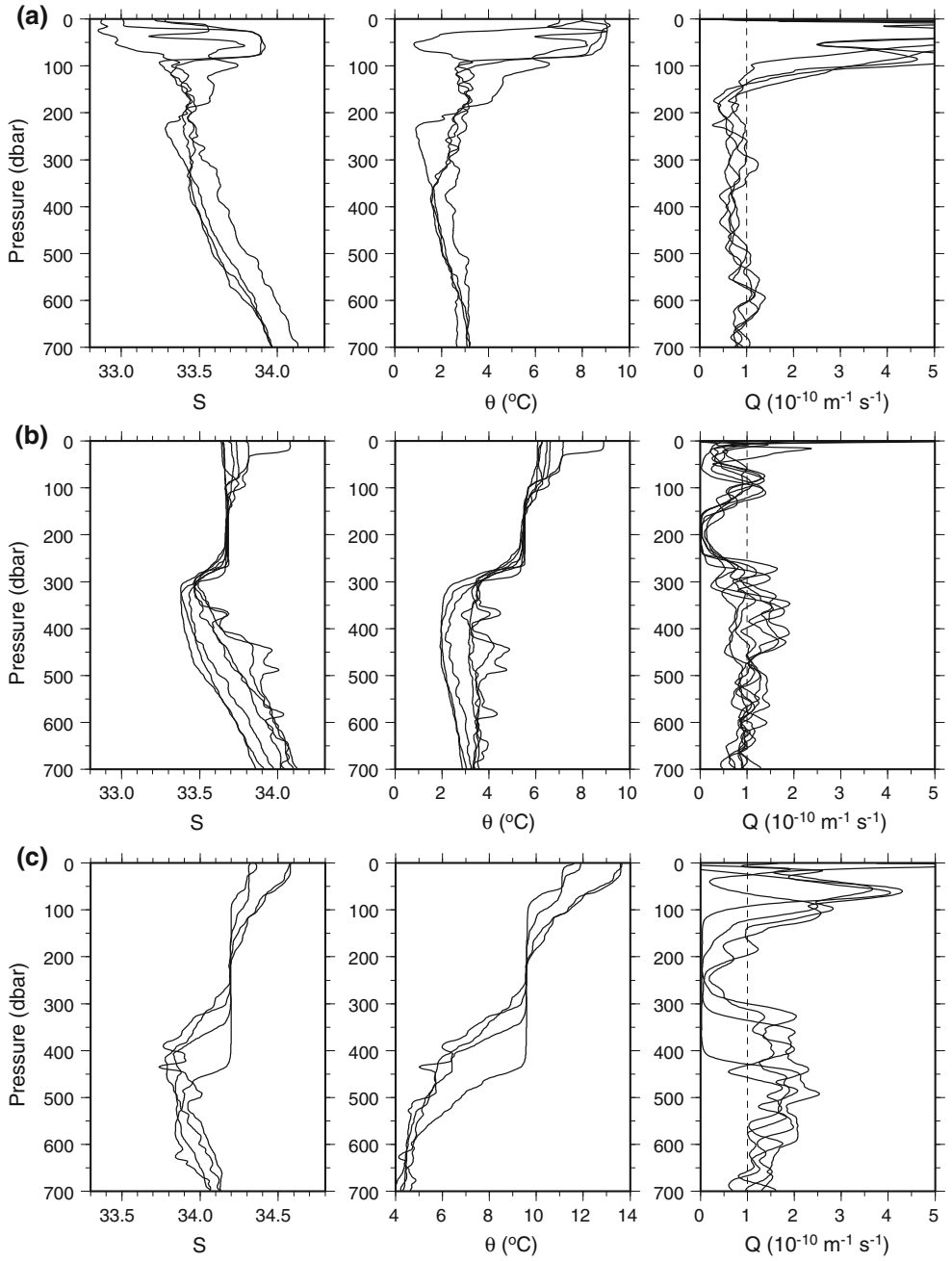

Fig. 7 Vertical profiles of (*left*) S, (*middle*) θ, and (*right*) Q obtained by the *Kofu-maru* at **a** four stations between 40.0° and 41.0°N along 144°E, **b** seven stations between 144.8° and 146.8°E along 40.25°N, and **c** four stations between 37.7° and 38.7°N, 148.5° and 149.2°E, in April 23–25 (**b**, **c**) and May 24 (**a**) of 2003. The locations of these stations are indicated by *dashed lines* in Fig. 6

region. West of 165°E, a group of CMW/TRMW pycnostads were found in only three areas: two anticyclonic eddies east of Japan (Sect. 4; Fig. 6) and an area south of SAFZ between 155° and 163°E. All three areas contained mode waters thicker than 200 dbar, which were not seen east of 165°E (Fig. 8b).

The southeastern eddy east of Japan contained pycnostads with uniform properties of $\sigma_\theta = 26.39$ kg m^{-3}, $\theta = 9.6$° C, and $S = 34.20$, which are characteristic of D-CMW (Figs. 7c, 8a, 9). The core Q of these D-CMW pycnostads was low ($0.02-0.18 \times 10^{-10}$ m^{-1} s^{-1}), implying that they were formed in late winter 2003, that is, a few months earlier than our observations. SSH data (not shown) indicate that the southeastern eddy was detached from the Kuroshio Extension in October 2002 and spent one winter before our observations in spring 2003. Past

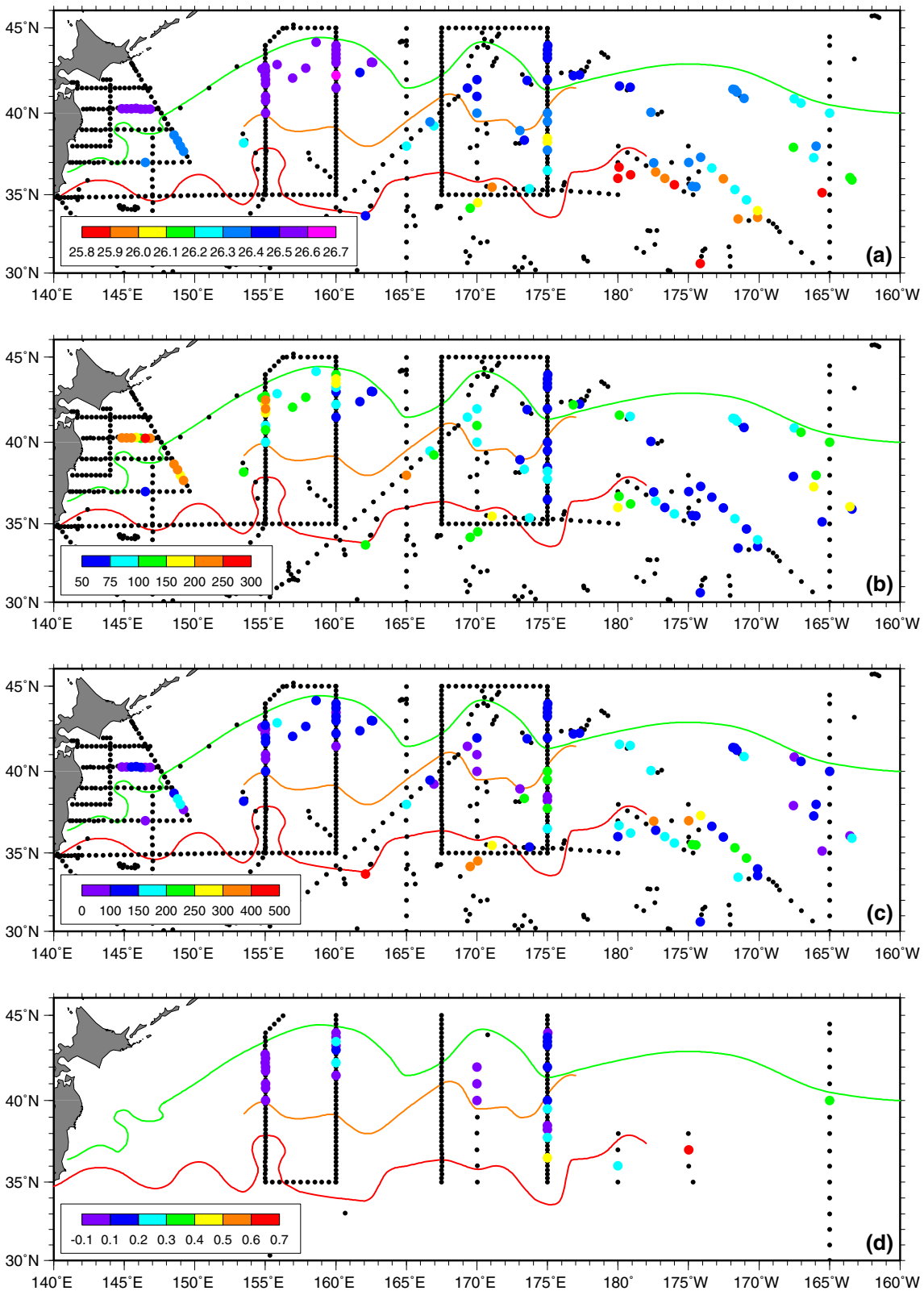
45°N
40°N
35°N
30°N
140°E 145°E 150°E 155°E 160°E 165°E 170°E 175°E 180° 175°W 170°W 165°W 160°W
25.8 25.9 26.0 26.1 26.2 26.3 26.4 26.5 26.6 26.7
(a)
50 75 100 150 200 250 300
(b)
0 100 150 200 250 300 400 500
(c)
-0.1 0.1 0.2 0.3 0.4 0.5 0.6 0.7
(d)

◀**Fig. 8** Distributions of **a** core σ_θ (kg m^{-3}), **b** thickness (dbar), **c** top depth (dbar), and **d** core AOU (ml l^{-1}) of L-CMW/D-CMW/TRMW pycnostads in spring 2003 (*color dots*). The observation points without a pycnostad are indicated by *black dots*. Plots in (**d**) are made only for CTD stations in the *Hakuho-maru* and *Shoyo-maru* cruises at which dissolved oxygen data were available. *Color curves* denote the fronts, as in Fig. 4

shipboard observations demonstrated that, inside an anticyclonic eddy pinched off from the Kuroshio Extension, STMW was modified to CMW or TRMW due to winter cooling and interaction with the ambient water (Tomosada 1986; Yasuda et al. 1992). The D-CMW held in the southeastern eddy might have been formed in a similar way. A pycnostad at 37°N, 146.5°E (Figs. 6, 8a) had exactly the same core properties as those in the southeastern eddy, which suggests that the pycnostad was formed in the eddy and then ejected from it.

The northwestern eddy held uniform TRMW pycnostads with $\sigma_\theta = 26.57$ kg m^{-3}, $\theta = 5.5°$ C, and $S = 33.68$ (Figs. 7b, 8a, 9). The core Q of these TRMW pycnostads was also low ($0.00-0.14 \times 10^{-10}$ m^{-1} s^{-1}), indicating that they were just formed in late winter 2003. The northwestern eddy lived for a long period from September 2001 to June 2005, drifting southeast of Hokkaido until summer 2004 and then propagating northeastward along the Kuril-Kamchatka trench, as described by Itoh and Yasuda (2010a) and Itoh et al. (2011). It was therefore supposed to have overwintered twice when observed in spring 2003, which probably made the contained mode water even cooler and fresher than that held in the southeastern eddy. According to the previous analysis of SSHA data (Itoh and Yasuda 2010b), anticyclonic eddies southeast of Hokkaido, including the northwestern one in our study, tend to propagate northeastward along the Kuril-Kamchatka trench, while those in the further offshore, including the southeastern one in our study, have a weak tendency to propagate northeastward along SAFZ. Hence, eddies such as the southeastern one might supply low Q to the broad TRMW formation region south of SAFZ mentioned below.

TRMW pycnostads with $\sigma_\theta = 26.49-26.61$ kg m^{-3}, $\theta = 5.7-7.3°$ C, and $S = 33.71-33.90$, which were similar to the properties of TRMW in the northwestern eddy, spread south of SAFZ at 40°–44°N, 155°–163°E (Figs. 2c, d, 8a, 9). They had relatively low core Q (0.44×10^{-10} m^{-1} s^{-1} on average), and their top is relatively shallow at 80–130 dbar (Fig. 8c). Furthermore, apparent oxygen utilization (AOU) at their core is mostly lower than 0.1 ml l^{-1} (Fig. 8d), which is characteristic of mode waters just after formation (Suga et al. 1989; Oka and Suga 2005). Based on these properties, these TRMW pycnostads were also judged to be formed in late winter 2003. Their locations correspond to where TRMW was discovered during the cruise in July 2002 (Saito et al. 2007) and to the location of the deepest winter mixed layer in the North Pacific appearing in the previous climatologies (Huang and Qiu 1994; Ladd and Thompson 2000; Suga et al. 2004). The reason why this area south of SAFZ is favorable for the TRMW formation is explained as follows. First, this area lies in a zonal band of lateral minimum in the vertical stability south of SAFZ, called the stability gap (Roden 1970, 1972; Yuan and Talley 1996), where neither the permanent thermocline characterizing the subtropical stratification nor the permanent halocline characterizing the subarctic stratification exists (Ladd and Thompson 2000; Suga et al. 2004; Fig. 2c). Secondly, a quasi-stationary jet associated with SAFZ (Isoguchi et al. 2006) brings warmer and saltier water from the south to this area, enhancing the oceanic heat loss and making the surface water denser in winter (Saito et al. 2007; Tomita et al. 2011). Actually, TRMW observed in spring 2003 was thickest about 100 km southeast of SAFZ (Fig. 8b), at which maximum oceanic heat loss in winter was observed (Tomita et al. 2011).

A TRMW pycnostad was also observed solely at 34°N, 162°E within KEF (Figs. 8a, 10). It had core σ_θ of

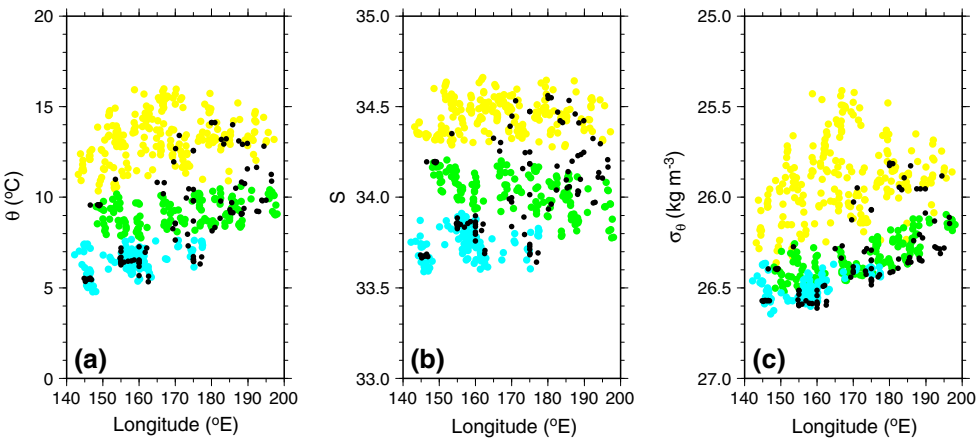

Fig. 9 Plots of **a** θ, **b** S, and **c** σ_θ against longitude (*black dots*) at the core of L-CMW/D-CMW/TRMW pycnostads. Background *dots* in *yellow*, *green*, and *blue* denote the properties of L-CMW, D-CMW, and TRMW, respectively, based on Argo float data in February–April of 2003–2008 (Oka et al. 2011a)

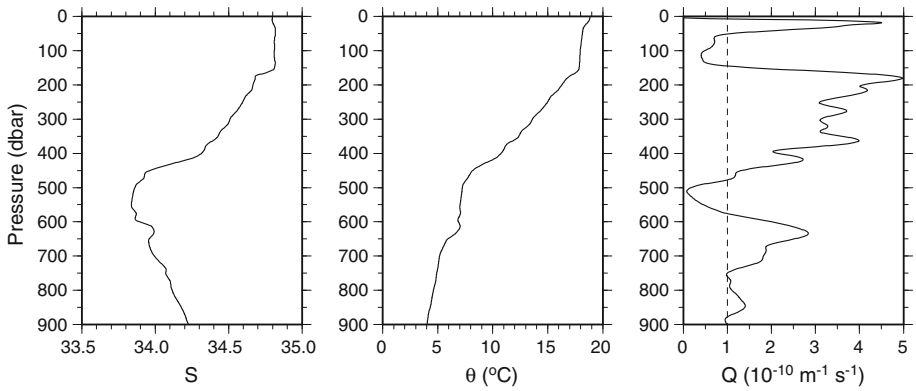

Fig. 10 Vertical profiles of (*left*) S, (*middle*) θ, and (*right*) Q obtained on May 21, 2003 by an Argo float at 33.7°N, 162.1°E

26.49 kg m^{-3}, core θ of 7.2 °C, and core S of 33.85, similar to those of TRMW pycnostads in the above formation area, and was relatively thick (=100 dbar), but was located more than 500 km south of the formation area and at depths of 480−580 dbar in the lower part of the main thermocline. Its low core Q (0.08 × 10^{-10} m^{-1} s^{-1}) suggests that it was formed in late winter 2003 and then subducted isopycnally to these depths across KBF and KEF. Such southward CMW/TRMW subduction across the fronts was pointed out by previous studies analyzing meridional hydrographic sections (Mecking and Warner 2001; Oka and Suga 2005). It might be related to the frontal instability (Spall 1995), and the subducted CMW as a form of subsurface mesoscale eddy can reach 1000 km south of KEF within 1 year from the formation (Oka et al. 2009). It should also be mentioned that the pycnostad at 34°N, 162°E corresponded to a vertical S minimum (Fig. 10), although its core σ_θ was lower than that of the North Pacific Intermediate Water (26.7−26.8 kg m^{-3}; Reid 1965; Talley 1993; Yasuda 1997). This might mean a possible contribution of the cross-frontal TRMW subduction to the NPIW formation around KEF (e.g., Yasuda et al. 1996).

East of 165°E, D-CMW and TRMW pycnostads were aligned zonally, with core σ_θ decreasing eastward and absence of TRMW east of 180° (Fig. 9), resembling the structure of these waters based on the 2003−2008 late winter Argo float data (Oka et al. 2011a). Just south of SAFZ, TRMW/D-CMW pycnostads with core σ_θ of 26.4−26.5 kg m^{-3} were located at 169°E−179°W, and D-CMW pycnostads with 26.3−26.4 and 26.2−26.3 kg m^{-3} were at 178°−171°W and 168°−165°W, respectively (Fig. 8a). Most of these pycnostads had a top depth of about 100 dbar (Fig. 8c), a low core AOU of 0.02−0.06 ml l^{-1} (Fig. 8d), and relatively low core Q (0.46 × 10^{-10} m^{-1} s^{-1} on average), and were judged to be formed in late winter 2003. These newly-formed TRMW/D-CMW pycnostads south of SAFZ, including those at 155°−163°E, were not particularly associated with anticyclonic eddies, as the observation points of these pycnostads were not related to strong maxima or minima of SSHA (Fig. 11). This suggests that the existence of stability gap, rather than eddies, is essential for the formation of these waters south of SAFZ. The zonal connection of these waters, particularly the influence of broad TRMW formation near 155°−163°E to the TRMW/D-CMW formation in the eastern (downstream) areas is not fully understood. Saito et al. (2011) analyzed Argo float data to indicate that the core θ and S of TRMW increase after spring due to double-diffusive salt-finger convection, which leads to the termination of TRMW at ∼180°.

Between 175° and 178°E, relatively thin TRMW pycnostads with core σ_θ = 26.4−26.5 kg m^{-3} were found north of SAFZ (Figs. 2g, 8a, b). They were shallow and had a low core AOU of 0.05−0.14 ml l^{-1} (Fig. 8c, d), and were considered to be locally formed in late winter 2003. Similar pycnostads north of SAFZ were observed in the repeat hydrographic section at 165°E (Oka and Suga 2005), although not observed at 165°E in spring 2003.

D-CMW pycnostads were also observed several degrees south of SAFZ. Those with core σ_θ = 26.3−26.4 kg m^{-3} located at 38°−40°N, 173°−175°E south of KBF had a low core AOU of 0.13−0.22 ml l^{-1}, but had a top depth of 200−210 dbar, which was larger than that (90−160 dbar) of majority of pycnostads (Figs. 2g, 8a, c, d). Since D-CMW is expected to be formed between KBF and SAF (Tsujino and Yasuda 2004; Oka and Suga 2005), these D-CMW pycnostads were believed to be formed north of KBF in late winter 2003 and then quickly subducted to the permanent pycnocline by crossing KBF southward. In the further downstream, D-CMW pycnostads with core σ_θ = 26.3−26.4 kg m^{-3} at 35°−37°N, 178°−175°W and those with 26.2−26.3 kg m^{-3} at 34°−36°N, 172−171°W were also deep, having a top depth of 230−340 dbar. One of these pycnostads at 37°N, 175°W had a core AOU of 0.64 ml l^{-1}, a typical value for mode waters formed more than a year ago (Oka and Suga 2005), which suggests that some of these pycnostads were formed in late winter 2002, unlike the other, newly formed pycnostads observed in spring 2003.

L-CMW is expected to be formed between KEF and KBF (Tsujino and Yasuda 2004; Oka and Suga 2005), but

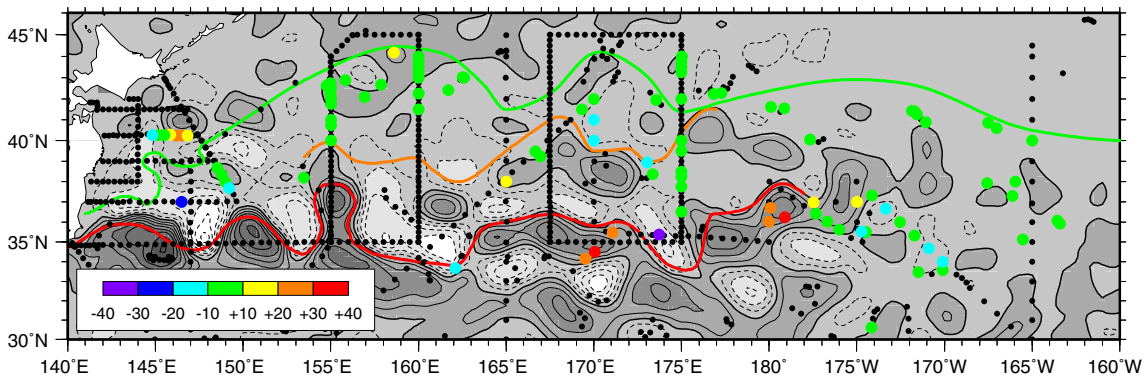

Fig. 11 Distributions of SSHA (cm; *color dots*) at the observation points of L-CMW/D-CMW/TRMW pycnostads in spring 2003. From weekly SSHA data, those closest in time to each observation were chosen and interpolated horizontally to obtain the SSHA value at the observation point. The *background contours* represent SSHA averaged in May–June. The contours are drawn at an interval of 10 cm, with thick contours at 0 cm and *darker shading* for larger values. *Red*, *orange*, and *green curves* denote KEF, KBF, and SAFZ, respectively

was hardly seen west of 165°E in spring 2003; the only L-CMW pycnostad with core σ_θ of 26.27 kg m^{-3}, core θ of 11.0° C, core S of 34.35, and relatively low core Q of 0.53×10^{-10} m^{-1} s^{-1} was observed at 38°N, 153°E (Figs. 8, 9). Between 165° and 175°E, L-CMW pycnostads, or pycnostads with properties between L-CMW and D-CMW, exhibited a patchy distribution, compared to the dense hydrographic observations. Those with core $\sigma_\theta = 26.2-26.4$ kg m^{-3} at 38°−39°N, 165°−167°E and those with core $\sigma_\theta = 26.0-26.3$ kg m^{-3} at 35°−38°N, 174°−175°E, located between KEF and KBF, were relatively shallow with a top depth of 90−210 dbar, while those with core $\sigma_\theta = 25.9-26.2$ kg m^{-3} at 34°−36°N, 169°−171°E in the recirculation south of KEF were deep with a top depth of 260−380 dbar, implying that they were subducted to the permanent pycnocline by crossing KEF southward. East of 180°, L-CMW pycnostads were shallow, had lower core σ_θ, and exhibited a more continuous distribution. Among them, those with core σ_θ of 25.82 kg m^{-3}, core θ of 14.1° C, core S of 34.55, and low core AOU of 0.23 ml l^{-1} at 36°−37°N, 180°−179°W were closely associated with an anticyclonic recirculation of the Kuroshio Extension, or an anticyclonic eddy that repeated detachment from and absorption by the Kuroshio Extension (Fig. 11). These pycnostads might be also converted from STMW through the winter of 2002/03, like D-CMW pycnostads held in the southeastern eddy east of Japan.

6 Discussion

The L-CMW/D-CMW/TRMW distributions in spring 2003 (Fig. 8a) were greatly different from those in the Argo-based 2003−2008 winter mixed layer climatology (fig. 4 of Oka et al. 2011a) in that D-CMW/TRMW was absent in the area east of Japan except in two anticyclonic eddies and that L-CMW hardly existed west of 165°E. The former fact indicates that, in the region north of SAFZ occupied by the cold and fresh Oyashio Water, mode water is formed mainly in anticyclonic eddies, which are detached from the Kuroshio Extension and carry the subtropical water. In the 2003−2008 winter mixed layer climatology, the TRMW/D-CMW formation region extends as far west as the east coast of Japan (Oka et al. 2011a). The western part of this formation region might be a composite of mode waters contained in eddies.

The absence of L-CMW west of 165°E might be related to the upstream KEF being in its stable state, which is characterized by low regional eddy activity (Qiu and Chen 2005). Since L-CMW, among the mode waters in the western North Pacific, exhibits the strongest relationship between its formation and eddies (Kouketsu et al. 2012), less frequent detachment of anticyclonic eddies from the stable upstream KEF, within which STMW can be modified to L-CMW (Tomosada 1986; Yasuda et al. 1992; Sect. 5), possibly resulted in the absence of L-CMW. Consistently, a recent analysis of Argo float data demonstrated that the winter mixed layer just north of the upstream KEF corresponding to the L-CMW formation region was significantly shallower during the stable KEF period of 2002−2005 and 2010−2011 than the unstable KEF period of 2006−2009 (Oka et al. 2012). This relationship was re-examined using more recent data from the fully developed Argo float network (Fig. 12). The winter mixed layer depth during the stable KEF period of 2010−2013 was shallower than 2006−2009 at 36°−40°N, 145°−155°E corresponding to the L-CMW formation region, although less noticeable than the difference in the STMW formation region south of KEF where the winter mixed layer is deeper during the

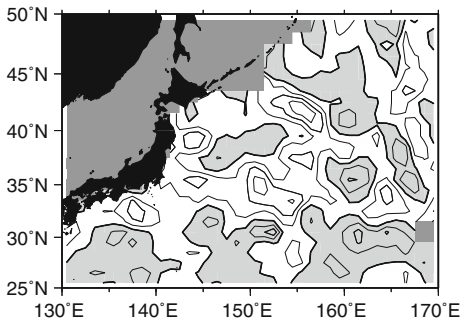

Fig. 12 Difference of the averaged mixed layer depth in February and March between 2010–2013 and 2006–2009 (former minus latter), calculated using Argo float data as in Oka et al. (2012; Fig. 4). The contour interval is 25 m, and negative values are *lightly shaded*. *Heavy shading* denotes *grid boxes* without data. Mixed layer depth for each Argo profile was calculated as the shallower value of the depth at which σ_θ increases by 0.03 kg m^{-3} from 10-dbar depth and that at which θ changes by 0.2° C from 10-dbar depth, following the definition of de Boyer Montégut et al. (2004) and Oka et al. (2007). Then, the mixed layer depth for each 4-year period was averaged for each 1° × 1° grid box using the Argo-based values from a 3° × 3° grid box centered by the 1° × 1° grid box and weight function of d^{-2} (d is a distance in degrees from the center of the 1° × 1° grid box) for observation points where $d > 1°$

stable KEF period, as demonstrated by Qiu and Chen (2006) and Qiu et al. (2007).

7 Summary

Temperature, salinity, and dissolved oxygen data from five research cruises and Argo profiling floats in spring 2003 were analyzed to examine the relationship of the CMW and TRMW formation in late winter 2003 to the thermohaline fronts and mesoscale eddies. The CMW/TRMW formation region east of Japan is delimited by three fronts. In spring 2003, KEF meandered at ~35°N from 140°E to a little beyond 180° (Fig. 4). KBF at ~40°N was identified between 155° and 175°E. SAFZ appearing as a single front extended northeastward from 36°N, 141°E to 44°N, 160°E and eastward farther east.

TRMW pycnostads with core $\sigma_\theta = 26.5-26.6$ kg m^{-3} were broadly formed just south of SAFZ between 155° and 163°E, as demonstrated by previous studies. TRMW and D-CMW pycnostads were also formed just south of SAFZ in the farther east up to 165°W, with core σ_θ decreasing eastward to 26.2 kg m^{-3} and absence of TRMW east of 180°. Such a TRMW/D-CMW formation was similar to that delineated using 2003−2008 late winter Argo float data (Oka et al. 2011a), and was not particularly associated with eddies, suggesting that the existence of stability gap is essential for the formation. D-CMW pycnostads were also observed several degrees south of SAFZ, which were much deeper than that just south of SAFZ, existing at depths more than 200 dbar. Most of these pycnostads were probably formed north of KBF in late winter 2003 and then quickly subducted to the permanent pycnocline by crossing KBF southward. This suggests that cross-frontal subducion transports a significant portion of D-CMW to the permanent pycnocline.

West of 155°E, TRMW and D-CMW were formed only in two anticyclonic eddies east of Japan, which differed significantly from the Argo-based picture, in which the formation region of CMW/TRMW extended as far west as the east coast of Japan (Oka et al. 2011a). TRMW with core $\sigma_\theta = 26.6$ kg m^{-3} was formed in a northwestern eddy that had spent at least two winters in this area, and D-CMW of 26.4 kg m^{-3} was formed in a southeastern eddy that was detached from the Kuroshio Extension in the previous fall. Within these eddies detached from the Kuroshio Extension, the contained subtropical water might have been modified to CMW and TRMW due to winter cooling and interaction with the ambient water, as demonstrated by previous studies.

L-CMW was hardly formed west of 165°E, which also differed significantly from the Argo-based picture. This might be related to the upstream Kuroshio Extension being in its stable state characterized by low regional eddy activity. Newly-formed L-CMW exhibited a patchy distribution between KEF and KBF at 165°−175°E and a more continuous distribution east of 180°. Some L-CMW pycnostads were subducted to the permanent pycnocline by crossing KEF southward, and some were formed in an anticyclonic eddy associated with the Kuroshio Extension.

The present analysis has demonstrated a clearer relationship of CMW/TRMW formation to the fronts and eddies than the previous studies. A re-analysis of accumulated Argo float data with SSH and SSHA data based on the present results will lead to further understanding of formation and subduction of these waters and their temporal variability. Additional high-resolution hydrographic sections (e.g., Oka et al. 2011b), particularly zonal ones, are also desired to clarify the modification of these waters within the formation region.

Acknowledgments The authors are grateful to the captain, crew, and scientists participating in the R/V *Kofu-maru* 0304 cruise, the R/V *Seifu-maru* 0304 cruise, and the R/V *Ryofu-maru* 0306 cruise of the Japan Meteorological Agency, the R/V *Hakuho-maru* KH-03-1 cruise of the Ocean Research Institute, The University of Tokyo, and the R/V *Shoyo-maru* FY2003 1st research cruise of the Fisheries Research Agency for their efforts in conducting the CTD and XCTD measurements. They also thank Tsuyoshi Ohira for his assistance in preparing the Argo float data and two anonymous reviewers for their helpful comments. The Argo float data used in this study were collected and made freely available by the International Argo Project and the national programs that contribute to it (http://www.argo.ucsd.edu, http://argo.jcommops.org). This study was initiated in 2005 when

E.O. was sent from Institute of Observational Research for Global Change, Japan Agency for Marine-Earth Science and Technology to Scripps Institution of Oceanography (SIO) as a visiting scholar. He thanks the late Nobuo Suginohara and Nobuyuki Shikama for giving him an opportunity to visit SIO. This study is supported by the Japan Society for Promotion of Science (KAKENHI, Grant-in-Aid for Scientific Research (B), No. 21340133 and 25287118) and the Ministry of Education, Culture, Sports, Science and Technology, Japan (MEXT; Grant-in-Aid for Scientific Research on Innovative Areas under Grant No. 22106007 and 25121502). Comments from participants at the "Research Meetings on Air-Sea Interaction" in 2011–2013 held as a part of the Collaborative Research Program of Hydrospheric Atmospheric Research Center, Nagoya University and at the research meeting "North Pacific Ocean Circulation and the Changes" in 2013 supported by the Atmosphere and Ocean Research Institute, The University of Tokyo and the Marine Meteorological Society of Japan were helpful.

References

Aoyama M, Hirose K, Nemoto K, Takatsuki Y, Tsumune D (2008) Water masses labeled with global fallout 137Cs formed by subduction in the North Pacific. Geophys Res Lett 35:L01604. doi:10.1029/2007GL031964

de Boyer Montégut C, Madec G, Fischer AS, Lazar A, Iudicone D (2004) Mixed layer depth over the global ocean: an examination of profile data and a profile-based climatology. J Geophys Res 109:C12003. doi:10.1029/2004JC002378

Ducet N, Le Traon PY, Reverdin F (2000) Global high-resolution mapping of ocean circulation from TOPEX/Poseidon and ERS-1 and -2. J Geophys Res 105:19477–19498

Freeland H et al (2010) Argo: a decade of progress. In: Hall J, Harrison DE, Stammer D (eds) Proceedings of OceanObs'09: Sustained Ocean Observations and Information for Society vol 2. 21–25 Sept 2009, ESA Publication WPP-306, Venice, Italy, doi:10.5270/OceanObs09.cwp.32

Hanawa K, Sugimoto S (2004) 'Reemergence' areas of winter sea surface temperature anomalies in the world's oceans. Geophys Res Lett 31:L10303. doi:10.1029/2004GL019904

Huang RX, Qiu B (1994) Three-dimensional structure of the wind-driven circulation in the subtropical North Pacific. J Phys Oceanogr 24:1608–1622

Ishii M, Inoue HY, Matsueda H, Saito S, Fushimi K, Nemoto K, Yano T, Nagai H, Midorikawa T (2001) Seasonal variation in total inorganic carbon and its controlling processes in surface waters of the western North Pacific subtropical gyre. Mar Chem 75:17–32

Isoguchi O, Kawamura H, Oka E (2006) Quasi-stationary jets transporting surface warm waters across the transition zone between the subtropical and the subarctic gyres in the North Pacific. J Geophys Res 111:C10003. doi:10.1029/2005JC003402

Itoh S, Yasuda I (2010a) Water mass structure of warm and cold anticyclonic eddies in the western boundary region of the subarctic North Pacific. J Phys Oceanogr 40:2624–2642

Itoh S, Yasuda I (2010b) Characteristics of mesoscale eddies in the Kuroshio–Oyashio Extension region detected from the distribution of the sea surface height anomaly. J Phys Oceanogr 40:1018–1034

Itoh S, Shimizu Y, Ito S, Yasuda I (2011) Evolution and decay of a warm-core ring within the western subarctic gyre of the North Pacific, as observed by profiling floats. J Oceanogr 67:281–293

Japan Meteorological Agency (2005) Data report of oceanographic and marine meteorological observations. No. 94, CD-ROM

Kawabe M (2005) Preliminary Report of the Hakuho Maru Cruise KH-03-1. Ocean Research Institute, The University of Tokyo

Kawai H (1972) Hydrography of the Kuroshio Extension. In: Stommel H, Yoshida K (eds) Kuroshio: its physical aspects. University of Tokyo Press, Tokyo, pp 235–352

Kobashi F, Kubokawa A (2012) Review on North Pacific subtropical countercurrent and subtropical front: role of mode water in ocean circulation and climate. J Oceanogr 68:21–43

Komaki K, Kawabe M (2009) Deep-circulation current through the main gap of the emperor seamounts chain in the North Pacific. Deep Sea Res I 56:305–313

Kono T, Kawasaki Y (1997) Modification of the western subarctic water by exchange with the Okhotsk sea. Deep Sea Res 44:689–711

Kouketsu S, Tomita H, Oka E, Hosoda S, Kobayashi T, Sato K (2012) The role of meso-scale eddies in mixed layer deepening and mode water formation in the western North Pacific. J Oceanogr 68:63–77

Ladd C, Thompson L (2000) Formation mechanisms for North Pacific central and eastern subtropical mode waters. J Phys Oceanogr 30:868–887

Levine ER, White WB (1983) Bathymetric influences upon the character of North Pacific fronts, 1976–1980. J Geophys Res 88:9617–9625

Masuzawa J (1969) Subtropical mode water. Deep Sea Res 16:463–472

Mecking S, Warner MJ (2001) On the subsurface CFC maxima in the subtropical North Pacific thermocline and their relation to mode waters and oxygen maxima. J Geophys Res 106:22179–22198

Midorikawa T, Ishii M, Nemoto K, Kamiya H, Nakadate A, Masuda S, Matsueda H, Nakano T, Inoue HY (2006) Interannual variability of winter oceanic CO_2 and air-sea CO_2 flux in the western North Pacific for 2 decades. J Geophys Res. 111:C07S02. doi:10.1029/2005JC003095

Mizuno K, White WB (1983) Annual and interannual variability in the Kuroshio current system. J Phys Oceanogr 13:1847–1867

Nakamura H (1996) A pycnostad on the bottom of the ventilated portion in the central subtropical North Pacific: its distribution and formation. J Oceanogr 52:171–188

Ohtani K (1971) Studies on the change of the hydrographic conditions in the Funka Bay. II. Characteristics of the waters occupying the Funka Bay. Bull Fac Fish Hokkaido Univ 22:58–66

Ohtani K (1989) The role of the Sea of Okhotsk on the Oyashio Water. Umi Sora 65:63–83 (in Japanese)

Oka E (2009) Seasonal and interannual variation of North Pacific subtropical mode water in 2003–2006. J Oceanogr 65:151–164

Oka E, Qiu B (2012) Progress of North Pacific mode water research in the past decade. J Oceanogr 68:5–20

Oka E, Suga T (2003) Formation region of North Pacific subtropical mode water in the late winter of 2003. Geophys Res Lett 30:2205. doi:10.1029/2003GL018581

Oka E, Suga T (2005) Differential formation and circulation of North Pacific central mode water. J Phys Oceanogr 35:1997–2011

Oka E, Talley LD, Suga T (2007) Temporal variability of winter mixed layer in the mid- to high-latitude North Pacific. J Oceanogr 63:293–307

Oka E, Toyama K, Suga T (2009) Subduction of North Pacific central mode water associated with subsurface mesoscale eddy. Geophys Res Lett 36:L08607. doi:10.1029/2009GL037540

Oka E, Kouketsu S, Toyama K, Uehara K, Kobayashi T, Hosoda S, Suga T (2011a) Formation and subduction of Central Mode Water based on profiling float data, 2003–08. J Phys Oceanogr 41:113–129

Oka E, Suga T, Sukigara C, Toyama K, Shimada K, Yoshida J (2011b) "Eddy-resolving" observation of the North Pacific subtropical mode water. J Phys Oceanogr 41:666–681

Oka E, Qiu B, Kouketsu S, Uehara K, Suga T (2012) Decadal seesaw of the central and subtropical mode water formation associated with the Kuroshio Extension variability. J Oceanogr 68:355–360

Ono T, Watanabe S, Okuda K, Fukasawa M (1998) Distribution of total carbonate and related properties in the North Pacific along 30°N. J Geophys Res 103:30873–30883

Qiu B, Chen S (2005) Variability of the Kuroshio Extension jet, recirculation gyre and mesoscale eddies on decadal timescales. J Phys Oceanogr 35:2090–2103

Qiu B, Chen S (2006) Decadal variability in the formation of the North Pacific subtropical mode water: oceanic versus atmospheric control. J Phys Oceanogr 36:1365–1380

Qiu B, Chen S (2011) Effect of decadal Kuroshio Extension jet and eddy variability on the modification of North Pacific intermediate water. J Phys Oceanogr 41:503–515

Qiu B, Chen S, Hacker P (2007) Effect of mesoscale eddies on subtropical mode water variability from the Kuroshio Extension System Study (KESS). J Phys Oceanogr 37:982–1000

Reid JL (1965) Intermediate Water of the Pacific Ocean. Johns Hopkins oceanographic studies, vol 2. John Hopkins University Press, Baltimore

Roden GI (1970) Aspects of the mid-Pacific transition zone. J Geophys Res 75:1097–1109

Roden GI (1972) Temperature and salinity fronts at the boundaries of the subarctic-subtropical transition zone in the western Pacific. J Geophys Res 77:7175–7187

Roemmich D, Johnson GC, Riser S, Davis R, Gilson J, Owens WB, Garzoli SL, Schmid C, Ignaszewski M (2009) Argo: the challenge of continuing 10 years of progress. Oceanography 22:46–55

Rossi V, Van Sebille E, Sen Gupta A, Garçon V, England MH (2013) Multi-decadal projections of surface and interior pathways of the Fukushima Cesium-137 radioactive plume. Deep Sea Res I 80:37–46

Saito H, Suga T, Hanawa K, Watanabe T (2007) New type of pycnostad in the western subtropical-subarctic transition region of the North Pacific: transition region mode water. J Oceanogr 63:589–600

Saito H, Suga T, Hanawa K, Shikama N (2011) The transition region mode water of the North Pacific and its rapid modification. J Phys Oceanogr 41:1639–1658

Shiozaki T, Ito SI, Takahashi K, Saito H, Nagata T, Furuya K (2013) Regional variability of factors controlling the onset timing and magnitude of spring algal blooms in the northwestern North Pacific. J Geophys Res 119:253–265. doi:10.1002/2013JC009187

Spall MA (1995) Frontogenesis, subduction, and cross-front exchanges at upper ocean fronts. J Geophys Res 100:2543–2557

Stabeno PJ, Ladd C, Reed RK (2009) Observations of the Aleutian North Slope Current, Bering Sea, 1996–2001. J Geophys Res 114:C05015. doi:10.1029/2007JC004705

Suga T, Hanawa K, Toba Y (1989) Subtropical mode water in the 137°E section. J Phys Oceanogr 19:1605–1618

Suga T, Takei Y, Hanawa K (1997) Thermostad distribution in the North Pacific subtropical gyre: the central mode water and the subtropical mode water. J Phys Oceanogr 27:140–152

Suga T, Motoki K, Aoki Y, Macdonald AM (2004) The North Pacific climatology of winter mixed layer and mode waters. J Phys Oceanogr 34:3–22

Sugimoto S, Hanawa K (2005) Remote reemergence areas of winter sea surface temperature anomalies in the North Pacific. Geophys Res Lett 32:L01606. doi:10.1029/2004GL021410

Sugiura J (1958) On the Tsugaru Warm Current. Geophys Mag 28:399–409

Talley LD (1988) Potential vorticity distribution in the North Pacific. J Phys Oceanogr 18:89–106

Talley LD (1993) Distribution and formation of North Pacific Intermediate Water. J Phys Oceanogr 23:517–537

Tomita H, Kouketsu S, Oka E, Kubota M (2011) Locally enhanced wintertime air-sea interaction and deep oceanic mixed layer formation associated with the subarctic front in the North Pacific. Geophys Res Lett 38:L24607. doi:10.1029/2011GL049902

Tomosada A (1986) Generation and decay of Kuroshio warm-core rings. Deep Sea Res 33:1475–1486

Tsujino H, Yasuda T (2004) Formation and circulation of mode waters of the North Pacific in a high-resolution GCM. J Phys Oceanogr 34:399–415

Uehara K, Ito S, Komatsu K (2004) Report of the R/V Shoyo-maru FY2003 1st research cruise. Fisheries Research Agency, Tokyo (in Japanese)

Yamashita Y, Tanoue E (2009) Basin scale distribution of chromophoric dissolved organic matter in the Pacific Ocean. Limnol Oceanogr 54:598–609

Yasuda I (1997) The origin of the North Pacific intermediate water. J Geophys Res 102:893–909

Yasuda I (2003) Hydrographic structure and variability of the Kuroshio–Oyashio transition area. J Oceanogr 59:389–402

Yasuda T, Hanawa K (1997) Decadal changes in the mode waters in the midlatitude North Pacific. J Phys Oceanogr 27:858–870

Yasuda I, Okuda K, Hirai M (1992) Evolution of a Kuroshio warm-core ring: variability of the hydrographic structure. Deep Sea Res 39:S131–S161

Yasuda I, Okuda K, Shimizu Y (1996) Distribution and modification of North Pacific Intermediate Water in the Kuroshio–Oyashio interfrontal zone. J Phys Oceanogr 26:448–465

Yuan X, Talley LD (1996) The subarctic frontal zone in the North Pacific: characteristics of frontal structure from climatological data and synoptic surveys. J Geophys Res 101:16491–16508

Zhang RX, Hanawa K (1993) Features of the water-mass front in the northwestern North Pacific. J Geophys Res 98:967–975